VIETNAM JOURNAL OF CHEMISTRY VOL. 52(5) 553-558 OCTOBER 2014
DOI: 10.15625/0866-7144 2014-0030

EFFECT OF ETHYLENE VINYL ACETATE COPOLYMER GRAFTED ACRYLIC ACID ON TENSILE PROPERTY, THERMAL STABILITY AND WEATHERABILITY OF EVA/SiO_2 NANOCOMPOSITES

Thai Hoang*, Nguyen Thuy Chinh, Nguyen Thi Thu Trang

Institute for Tropical Technology, Vietnam Academy of Science and Technology

Received 29 July 2014; Accepted for Publication 15 October 2014

Abstract

In this work, the ternary nanocomposites (EGSC) were prepared based on ethylene vinyl acetate copolymer (EVA), ethylene vinyl acetate copolymer grafted with acrylic acid (EVAg) and silica nanoparticles (SiO_2) by melt mixing method. The effect of different content of EVAg on relative melt viscosity, thermal stability and weatherability of EGSC were investigated. The relative melt viscosity was determined by Polylab 3.1 software connected to intermixer Haake Rheomixer. The interfacial interactions of SiO_2 phase and EVA phase in EGSC were evaluated by Fourier Transform Infrared Spectroscopy (FTIR) through the wavenumber shifts of characterized groups in EGSC compared to EVA, EVAg, SiO_2 and Scanning Electron Microscopy images observation of EVA/SiO_2 nanocomposites with and without EVAg. The tensile strength and elongation at break of EGSC were significantly enhanced when adding EVAg into EVA/SiO_2 nanocomposite (ESC), especially at the ESC containing 1 wt.% EVAg. The improvement of EVAg on thermal stability and weatherability of ESC were also discussed.

Keywords: EVA, SiO_2, EVA grafted with acrylic acid, tensile property, thermal stability, weatherability.

1. INTRODUCTION

Ethylene vinyl acetate copolymer (EVA) is extensively used for the application of electrical insulation purpose, cable jacketing and repair, component encapsulation and water proofing, corrosion protection and packaging owing to its good physical and mechanical properties [1, 2]. However, like most of other organic polymers, EVA is also combustible and has low weatherability, limiting its application [2, 3]. In order to overcome these problems, many researchers have used various methods to improve mechanical properties, thermal stability and solvent resistance of EVA such as high-energy irradiation (^{60}Co γ-rays and electron beam), usage of inorganic filler, organosilane and chemical cross-linking [4-7]. Inorganic nanoadditives: nanosilica and nanoclay are able to enhance the properties of EVA and EVA-based nanocomposites. They are more widely used because of their excellent heat-resistance, tensile and toughness properties, etc. Unfortunately, silica is poor to disperse and adhere with EVA matrix. Therefore, using a compatibilizer to improve the interfacial adhesion between silica phase and EVA matrix is very necessary. In our previous works, the effect of nanosilica and ethylene vinyl acetate copolymer grafted with maleic anhydride (EVAgMA) as a compatibilizer on relative melt viscosity, morphology, structure and properties of EVA was studied [8, 9]. It was clear that mechanical properties and relative melt viscosity of EVA were improved by using 1.5 wt.% nanosilica (in comparison with EVA weight), and the important role of EVAgMA compatibilizer in EVA/silica nanocomposites was approved.

Until now, the effect of ethylene vinyl acetate copolymer grafted with acrylic acid (EVAg) on some properties and morphology of EVA/SiO_2 nanocomposites have not been studied yet. This work reports results of study on relative melt viscosity, thermal stability and weatherability of EVA/SiO_2 nanocomposites containing different content of EVAg.

2. EXPERIMENTAL

2.1. Materials

Ethylene vinyl acetate copolymer (EVA) containing 10 wt.% vinyl acetate in granular form with the density of 0.93 $g.cm^{-3}$ and melt flow index

of 1.3 g/10min /190°C/2.16 kg was purchased from Hanwha Co., South Korea. Silica nanoparticles (SiO_2) with purity of 99.8 %, average particle size of 12 nm, acrylic acid and dicumyl peroxide were provided by Sigma-Aldrich Co. (USA).

2.2. Preparation of EVA/silica nanocomposites

EVA grafted with acrylic acid (EVAg) was prepared by melt mixing EVA, acrylic acid (AA) and DCP in the Haake Rheomixer (content of AA grafted to EVA is 1 wt.% compared to EVA weight). The nanocomposites containing 1.5 wt.% of SiO_2 (SiO_2 optimum content as found at [8]) and 0; 0.5; 1; 1.5; 2 wt.% of EVAg (compared to EVA weight) were also prepared by melt mixing at temperature of 160 °C in 5 minutes and rotor speed of 50 rpm. After melt mixing, the nanocomposites were molded by hot pressured machine (Toyoseky, Japan) at 160°C with 15 MPa pressure for 3 minutes to form the samples with thickness about 1 mm. The EVA/EVAg/SiO_2 nanocomposites with 0; 0.5; 1; 1.5; 2 wt.% of EVAg were abbreviated by ESC; EGSC0.5; EGSC1; EGSC 1.5 and EGSC2, respectively.

2.3. Characterization

Imitation of the relative melt viscosity in mixing process was carried out by a Haake Rheomixer using Polylab 3.1 software. Fourier Transform Infrared spectra (FTIR) were recorded on a FTIR-Nexus infrared spectrometer using thin films of the samples in the range of 4000-400 cm^{-1} at room temperature. Tensile properties such as tensile strength and elongation at break of the nanocomposites were measured on a Zwick Tensile 2.5 Machine according to the ASTM D638 standard. Morphology of the nanocomposites was analyzed by using an S-4500 Scanning Electron Microscopy (SEM) (Hitachi). Thermal property studies were performed by a DTG-60H thermogravimetric analyzer (Shimadzu Co.) under argon atmosphere from room temperature to 600 °C and at a heating rate of 10°C/min. Accelerated weathering test was carried out on UV-CON 327 (USA) to evaluate the weartherability of the nanocomposites. Every cycle of the accelerated weathering test includes: 8 hours of UV irradiation at 60°C and 4 hours of humidity condensate at 45°C. Total testing time is 168 hours (corresponding to 14 cycles). The tensile properties of the nanocomposites were determined before and after 8 and 14 cycles of accelerated weathering test.

3. RESULTS AND DISCUSSION

3.1. Relative melt viscosity

Figure 1 describes torque curves expressed melt process of ESC and EGSC samples with similar shapes. Before one minute of mixing, the torque curves of samples have the maximum peak due to polymer is still at solid state. Then, the torque of the samples decreases and at about four minutes of mixing, the torque of all samples achieves to stable value or "equilibrium". Clearly, the torque of the EGSC samples is lower than that of ESC due to the chains of EVA and AA moieties in EVAg can be easily mixed with EVA matrix. EVAg increases mobility of EVA chains and decreases interfacial interaction of SiO_2 nanoparticles [1, 2]. The stable torque of ESC and EGSC samples which was recognized from 4th to 5th minute of melt mixing process is presented in Table 1. The obtained result also shows that the stable torque decreased as increasing the EVAg content.

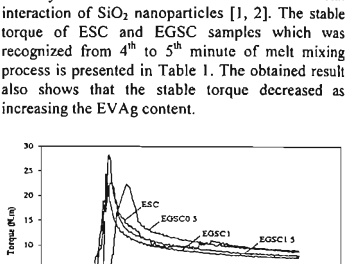

Fig. 1: Torque curves of ESC and EGSC samples

Table 1: Stable torque of ESC and EGSC samples

Samples	Stable torque (N.m)
ESC	9.15
EGSC0.5	9.10
EGSC1	8.05
EGSC1.5	8.25

3.2. FTIR spectroscopy

FTIR spectra of EVA, EVAg, SiO_2 and EGSC1 are shown in Fig. 2. The FTIR spectra of EGSC0.5, EGSC1.5 and EGSC2 are similar to spectrum of EGSC1, thus, they are not shown here. The peaks at 3448, 2921, 2847, 1110, 955, 794, 461 cm^{-1} can be attributed to the characterized absorption bands of OH, methylene and Si-O of SiO_2 groups,

respectively. The typical absorption peaks of EVA include 2924 cm^{-1} (C-H stretching vibration), 1737 cm^{-1} (C=O stretching vibration), 1456 cm^{-1}, 1368 cm^{-1} and 724 cm^{-1} (C-H bending vibration), 1242 cm^{-1} (C-O-C asymmetric stretching vibration), and 1025 cm^{-1} (C-O-C symmetric stretching vibration). In comparison to EVA spectrum, the EVAg spectrum has one new peak characterized for stretching vibration of OH group and the slight shifts of the peaks (1-7 cm^{-1}) which prove the formation of interactions between AA and EVA after grafting. The strong shifts of peaks of Si-O stretching and bending vibration (5-17 cm^{-1}), C=O stretching vibration (12-13 cm^{-1}) and C-O-C stretching vibration (5-10 cm^{-1}) indicated that interfacial interactions including hydrogen bonds and dipole-dipole interactions between OH on the surface of SiO_2 and C=O and C-O-C groups of EVAg and EVA [9-11].

Table 1: The characterized wavenumbers of EVA, SiO_2, EVAg and EGSC1 samples

Samples	Wavenumbers, cm^{-1}								
	ν_{OH}	ν_{CH}	$\nu_{C=O}$	δ_{CH}	ν_{C-O}	ν_{Si-O}	ν_{Si-OH}	γ_{CH}	δ_{Si-O}
SiO_2	3448	2921 2847				1110 794	955		461
EVA		2924	1737	1456 1368	1242 1025			724	
EVAg	3500	2921 2852	1738	1463 1370	1241 1021			723	
EGSC1	3612 3456	2925	1725	1457 1368	1238 1011	1127 806	963	720	450

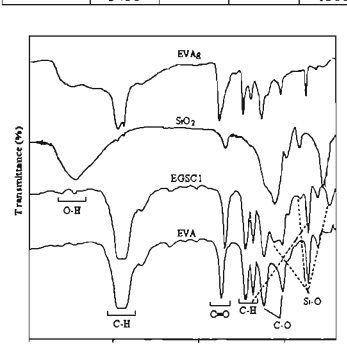

Fig. 2: FTIR spectra of EVA, EVAg, SiO_2, EGSC1 samples

respectively. There is a slight weight loss in the first decomposition step, which may be ascribed to the

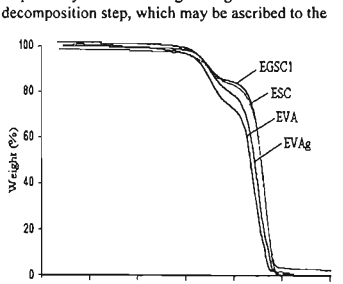

Fig. 3: TGA diagrams of EVA, EVAg, ESC and EGSC samples

3.3. Thermal stability

Thermogravimetric (TG) diagrams of EVA, ESC and EGSC samples are demonstrated in Fig. 3. It is clear that thermal degradation of all samples includes three steps, in the temperature (T) ranges about 210-300 °C, 310-385 °C and 410-496 °C, formation of ester mixtures (T< 280 °C) and the charring layer, compared to the sharp weight loss of the two rest steps [1]. At the two following weight loss processes, the weight loss of EGSC samples in the second and third decomposition steps is slower than that of EVA. When using EVAg, thermal degradation rate of the nanocomposites in the second step is slower than that of EVA. According

to the previous reports [1, 2, 9], thermal degradation of neat EVA proceeds mainly by the following mechanism: the loss of acetic acid (310–385°C) forming unsaturated polyenes and then the random chain scission of the hydrocarbon chains of EVA producing unsaturated vapor species (410–496°C), such as butane and ethylene [1, 2, 9]. The TG characteristics of EVA, ESC and EGSC samples are described in Table 2. The temperature corresponding to the onset of thermal decomposition for a polymer is essential for evaluating its thermal stability. From table 2, it can be seen that the onset temperature (T_0) and maximum degradation temperature (T_{max}) of the nanocomposites significantly increases in comparison to EVA. The addition of EVAg leads to a strong shift in T_0 and T_{max} of EGSC samples to a higher temperature.

Table 2: TG characteristics of EVA, ESC and EGSC samples

Samples	T_0 (°C)	T_{max1} (°C)	T_{max2} (°C)	The percent of weight retention (%)		
				350 °C	400 °C	450 °C
EVA	269	351	446	86.3	72.7	28.0
EVAg	276	354	456	89.8	78.9	41.6
ESC	283	352	468	90.3	83.3	62.8
EGSC0.5	288	353	468	90.8	83.9	63.5
EGSC1	291	354	467	91.2	84.5	64.3
EGSC1.5	290	352	467	91.0	84.1	63.1

T_0: the onset temperature; T_{max}: the maximum degradation temperature.

3.4. Weatherability

3.4.1. The tensile properties of EVA/SiO_2 nanocomposites before weathering test

As mentioned in the reference [8], the tensile strength and elongation at break of EVA/SiO_2 nanocomposites are strongly affected by dispersion and adhesion of SiO_2 in EVA matrix. When EVAg as a compatibilizer with suitable content is added to the nanocomposites, the interfacial interaction between SiO_2 and EVA is improved. It contributes to decrease SiO_2 particle agglomerates. As a result, the tensile strength and elongation at break of the EGSC samples are enhanced, especially for EGSC1 sample (Fig. 4). With 1 wt.% of EVAg, the tensile strength of EGSC reaches the highest value.

3.4.2. The tensile properties of EVA/SiO_2 nanocomposites after weathering test

The remained percent of tensile property of EGSC samples after 96 and 168 hours of accelerated weathering test is higher than that of ESC, especially EGSC1 sample (Fig. 5). It can be explained by EVAg playing an important role in improvement of compatibility between EVA and SiO_2 phases. Besides, the appearance of new peak at about 1640 cm^{-1} and shoulder at about 1750 cm^{-1} is related to the new types of the carbonyl groups formation such as ketone, lactone carbonyl and aliphatic ester (Fig. 6) [12]. It exhibits rearrangement in crystalline region of samples after weathering test.

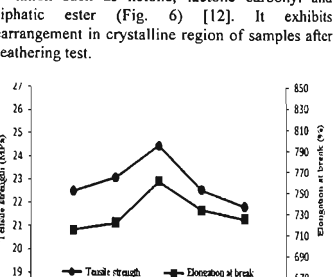

Fig. 4: The tensile properties of ESC and EGSC samples

SEM images of the surface of EVA, ESC and EGSC1 after accelerated weathering test are shown in Fig. 7. Observably, EVAg increased SiO_2 phase fine dispersion in EVA matrix and interfacial adhesion between the phases. The smaller size and more regular dispersion of SiO_2 in EVA matrix

contribute to limit photooxidation degradation of EVA due to barrier ability against oxygen penetration, humidity and high temperature. As a result, the formation of carbonyl, carboxyl, and hydroperoxide groups, reactive radicals, polymers chains scission can be decreased [13-15]. Thus, it can see the number of cracks and holes on the surface of EGSC1 sample is reduced and their size, area are smaller than those of EVA and ESC at the same time of accelerated weathering test. This can explain for increase of weatherability of EVA/SiO_2 nanocomposites using EVAg as a compatibilizer with the EVAg content of 0.5, 1, and 1.5 wt.%.

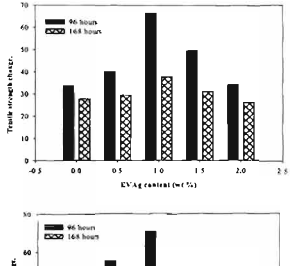

Fig. 5: The tensile property retention of EGSC samples

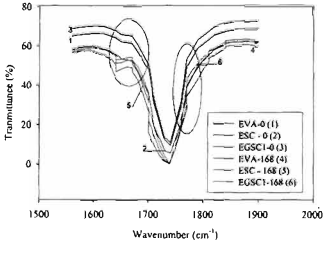

Fig. 6: The FTIR of EGSC samples before and after 168 hour of accelerated weathering test

4. CONCLUSION

In this paper, the important role of EVAg for improvement properties of EVA/SiO_2 nanocomposites was proved. By hydrogen bonds and dipole-dipole interactions connecting SiO_2 with EVA matrix via EVAg, an enhancement for tensile strength, elongation at break, thermal stability and weatherability is observed for EGSC samples. The obtained results also indicate that 1 wt.% of EVAg is the most suitable content to prepare EVA/SiO_2 nanocomposites.

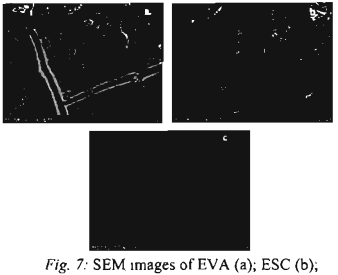

Fig. 7: SEM images of EVA (a); ESC (b); EGSC1(c) samples after 168 hour accelerated weathering test

Acknowledgements. *The authors would like to thank the National Foundation for Science and Technology Development of Vietnam (104.04-2010.02) for the financial support.*

REFERENCES

1. B. B. Wang, X. F. Wang, Y. Q. Shi, G. Tang, Q. B. Tang, L. Song, Y. Hu. Radiat. Phys. Chem., **81**, 308 (2012).
2. A. Vallés-Lluch, G. Gallego Ferrer, M. Monleón Pradas. European Polymer Journal, **46(5)**, 910 (2010).
3. C. M. Jiao, Z. Z. Wang, X. L. Chen, B. Y. Yu, Y. Hu, Radiat. Phys. Chem., **75(5)**, 557 (2006).
4. B. Li, H. Jia, L. M. Guan, B. C. Bing, J. F. Dai, J. Appl. Polym. Sci., **114(6)**, 3626 (2009).
5. H. Liu, Z. P. Fang, M. Peng, L. Shen, Y. C. Wang. Radiat. Phys. Chem., **78(8)**, 922 (2009).
6. B. B. Wang, L. Song, N. N. Hong, Q. L. Tai, H. D. Lu, Y. Hu. Radiat. Phys. Chem., **80(11)**, 1275 (2011).
7. R. Scaffaro, L. Botta, G. Gallo. Polymer Degradation and Stability, **97**, 653 (2012).

8. T. Hoang, N. T. Chinh, B. N. Son, N. T. Thu Trang. Vietnam Journal of Science and Technology, **50(1B)**, 547 (2012).

9. T. Hoang, N. T. Chinh, D. Q. Tham, D. T. Mai Thanh, T. A. Truc, N. T. Thu Trang, N. V. Giang and T. D. Lam, KGK, 6 June (2011) 3493 (2012).

10. J. H. Chen, M. Z. Rong, W. H. Ruan, M. Q. Zhang. Composites Science and Technology, **69**, 252 (2009).

11. D. N. Bikiaris, A. Vassiliou, E. Pavlidou, G. P. Karayannidis. European Polymer Journal, **41**, 1965 (2005).

12. I. S. Suh, S. H. Ryu, J. H. Bae, Y. W. Chang. Journal of Applied Polymer Science, **94(3)**, 1057, (2004).

13. J. Jin, S. Chen, J. Zhang, Polymer Degradation and Stability, **95**, 725 (2010).

14. T. Hoang, N. T. Chinh, N. T. Thu Trang, D. T. Mai Thanh, D. V. Hung, C. S. Ha, M. Aufray. Macromolecules Research, **21** (2013).

15. S. Hui, S. Chattopadhyay, T. K. Chaki. Polymer Composites, **31(8)**, 1387 (2010).

Corresponding author: **Thai Hoang**
Institute for Tropical Technology,
Vietnam Academy of Science and Technology
18 Hoang Quoc Viet Road, Cau Giay District, Hanoi, Vietnam
E-mail: hoangth@itt.vast.vn.